Supplementary Materials

3D flower-like CuO@NiAl-LDH microsphere with enhanced removal affinity to organic dyes: Mechanistic insights, DFT calculations and toxicity assessment

Yao Chen[1], Honglin Lian[1], Hao Wang[1], Jun Qin[3], Xiaolang Chen[1, 2, *], Zongcheng Lu[2]

1. Key Laboratory of Advanced Materials Technology Ministry of Education, School of Materials Science and Engineering, Southwest Jiaotong University, Chengdu 610031, China;

2. Sichuan Jiahe Copolymerization Science and Technology Co. Ltd., Chengdu 610015, China;

3. Key Laboratory of Karst Georesources and Environment, Ministry of Education, College of Resources and Environmental Engineering, Guizhou University, Guiyang 550025, China.

*Corresponding author, E-mail address: chenxl612@ sina.com (X. L. Chen).

List of text, table and figures

Text S1: Calculation details

The computational calculations based on density functional theory (DFT) calculations in this work were calculated with Gaussian 09 software [1]. The B3LYP-D3(BJ) theoretical method using 6-31G(d) basis were executed to predict the geometry optimization of methylene blue (MB) molecular. Furthermore, Fukui function has long been used as an effective way to predict reactive active sites of electrophilic, nucleophilic and radical attack, which is an important concept in the conceptual density functional theory (DFT). What's more, Hirshfeld charges, condensed Fukui functions (the nucleophilic (f^+), electrophilic (f^-) and radical attack (f^0)), the lowest unoccupied molecular orbits (LUMO), the highest occupied molecular orbits (HOMO) and surface electrostatic potential (ESP) of MB were calculated with Multiwfn 3.8 (dev) at B3LYP/6-31G(d) level and then the electrostatic potential on the molecular surface is plotted with Visual Molecular Dynamics (VMD version 1.9.3) [2].

Notably, Fukui function is displayed as:

$$f(r) = \left(\frac{\partial^2 E}{\partial N.\partial v(r)}\right) = [\frac{\partial \mu}{\partial v(r)}]_N = [\frac{\partial \rho(r)}{\partial N}]_{V(r)} \quad (1)$$

where $\rho(r)$ is the electron density at a point *r* in space, *N* is electron number in present system, the constant term *v* in the partial derivative is external potential. In the condensed version of Fukui function, atomic population number is used to represent the amount of electron density distribution around an atom.

Then the condensed Fukui function including can be calculated by following functions:

Electrophilic attack: $f_A^- = q_{N-1}^A - q_N^A$ (2)

Nucleophilic attack: $f^{+}_{A} = q^{A}_{N} - q_{N}{}^{A}_{+1}$ (3)

Radical attack: $f^{0}_{A} = (q_{N}{}^{A}_{-1} - q_{N}{}^{A}_{+1})/2$ (4)

where q^{A} is the atom charge of atom A at the corresponding state, f_{A} represents the Fukui value of atom A.

Text S2: Toxicity assessment

The toxicity of MB and its degradation intermediates are predicted with the aid of the Toxicity Evaluation Software Tool (T.E.S.T.). Six indicators of mutagenicity, developmental toxicity, bioaccumulation factor, acute toxicity of fathead minnow LC50 (96 h), T. pyriformis IGC50 (48 h), and daphnia magna LC50 (48 h) are predicted based on quantitative structure-activity relationship (QSAR, to predict measures of toxicity from physical characteristics of the structure of chemicals) methods [3]. T.E.S.T to estimate toxicity values using several different advanced QSAR methodologies. In T.E.S.T estimating toxicity values we mainly utilized Consensus method and Hierarchical clustering method QSAR methodologies.

Consensus method: The predicted toxicity is estimated by taking an average of the predicted toxicities from QSAR methods.

Hierarchical clustering method: The toxicity for a given query compound is estimated using the weighted average of the predictions from several different models. The different models are obtained by using Ward's method to divide the training set into a series of structurally similar clusters. A genetic algorithm-based technique is used to generate models for each cluster. The models are generated prior to runtime.

Table S1 Comparison of Fenton-like MB removal using various catalysts

Catalytic material	Experimental conditions				Removal		Stability		Refs.
	Catalyst (g/L)	MB (mg/L)	H_2O_2 (mmol/L)	pH	efficiency (%)	Time (min)	cycles	reduction after cycles (%)	
Fe-Cu-080	0.5	5	500	7	99	60	6	4	[4]
Au/ZnO	1	15	500	7.5	90	120	3	35.9	[5]
CNCOF	1.25	20	80	5	100	20	10	13	[6]
Fe(II)-doped g-C_3N_4	0.5	50	200	6.5	100	90	4	1	[7]
HKUST-1/Fe_3O_4/CMF	0.33	10	118	3	98	240	5	6.5	[8]
$ZnNb_2O_6$	1	15	500	5.2	97.8	300	-	-	[9]
Fe_3O_4/CeO_2	1	100	170	6	100	120	-	-	[10]
Fe_3O_4/C octahedra	0.5	10	90	3	100	120	10	3	[11]
Yolk-shell Fe_3O_4@MOF-5	1	50	30	4	100	90	5	2	[12]
HC-ZVI	0.4	10	100	6.4	97.77	80	3	25.31	[13]
MnMgFe-LDH	2	20	100	7	92	300	5	12	[14]
Fe_3O_4/SiO_2/C	1	100	480	6	90	60	8	25	[15]
Fe_3O_4@NIP	1	25	300	6.9	99	300	5	5	[16]
CuO@LDH-5	1	10	100	6	99	120	5	14	This work

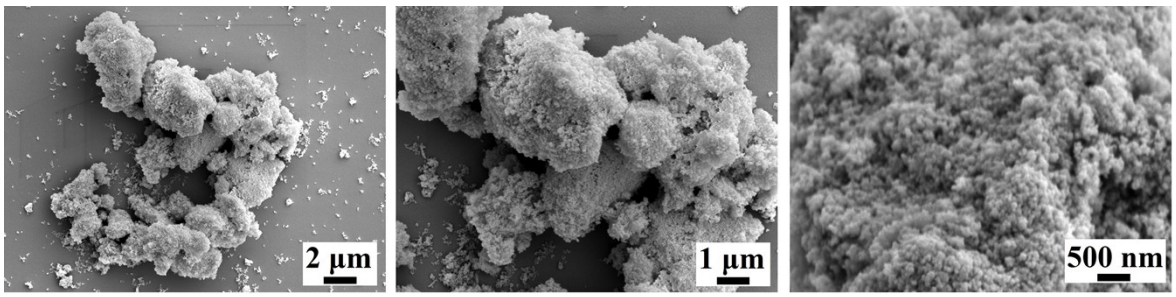

Fig. S1 The SEM images of CuO.

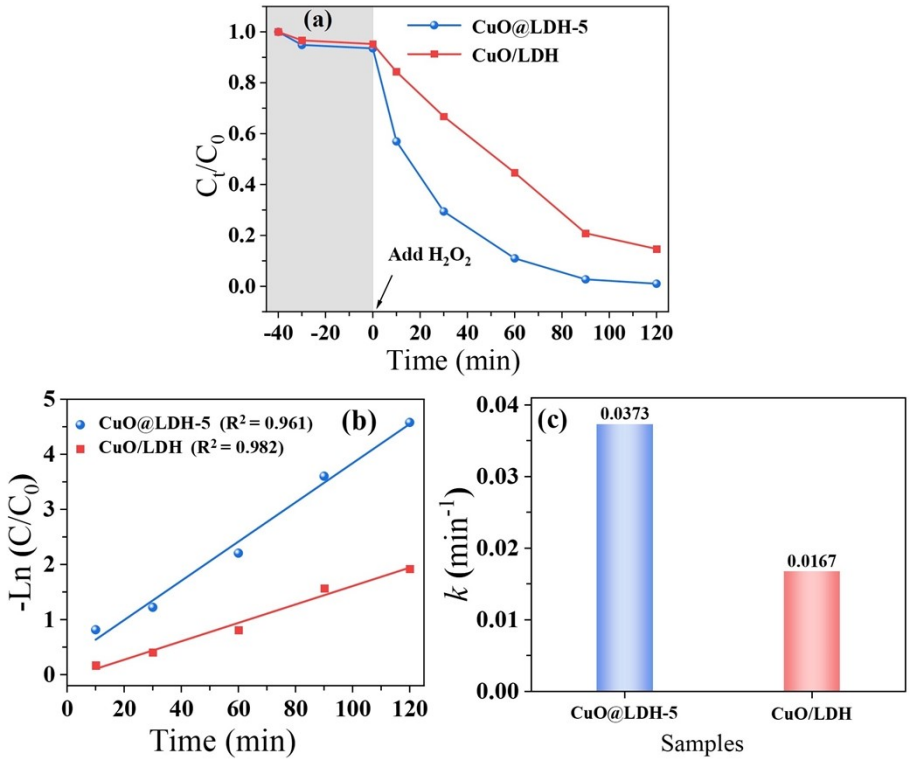

Fig. S2 (a) The performances of CuO@LDH-5 and the physical mixture of CuO and LDH; (b) Kinetic analysis of MB in the degradation process; (c) Degradation rate constants *k*. (Experimental conditions: catalyst dosage = 1 g/L, initial pH = 6, MB concentration = 10 mg/L, H_2O_2 concentration = 100 mM).

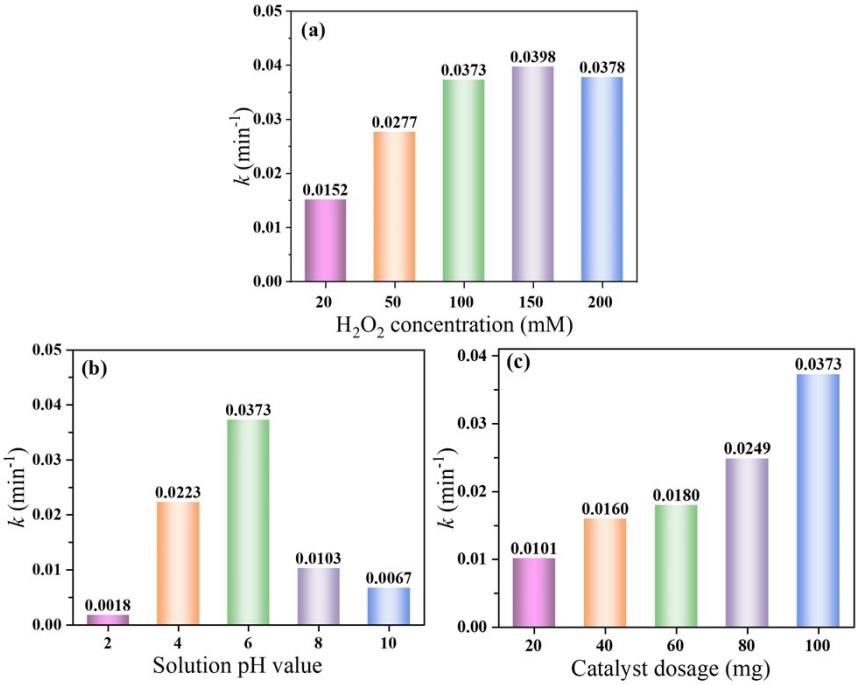

Fig. S3 Degradation rate constants *k* of different experimental conditions on the degradation performances for MB in CuO@LDH-5 with H_2O_2 systems: (a) H_2O_2 dosage, (b) solution pH, and (c) catalyst dosage. (In addition to the specific parameters, the experimental conditions were as follows: catalyst dosage = 1 g/L, initial pH = 6, MB concentration = 10 mg/L, H_2O_2 concentration = 100 mM).

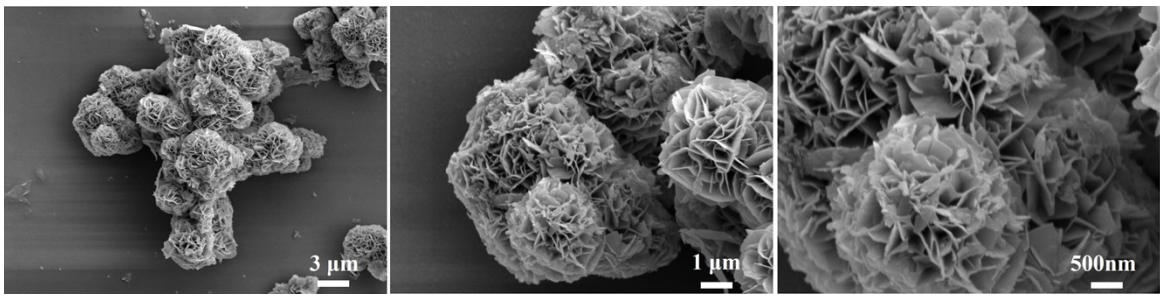

Fig. S4 The SEM images of used CuO@LDH-5

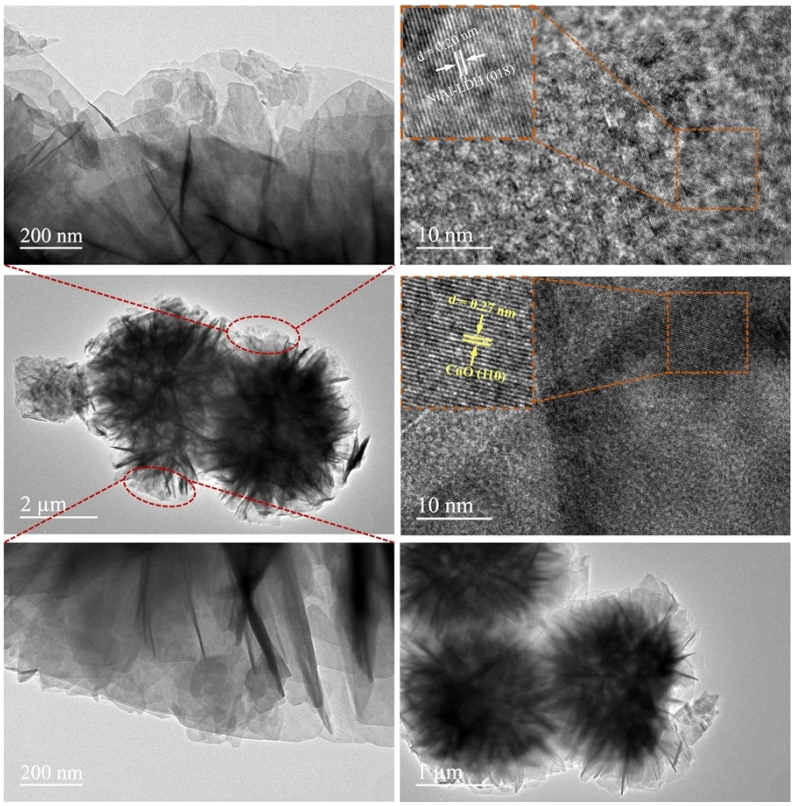

Fig. S5 The TEM and HRTEM images of used CuO@LDH-5.

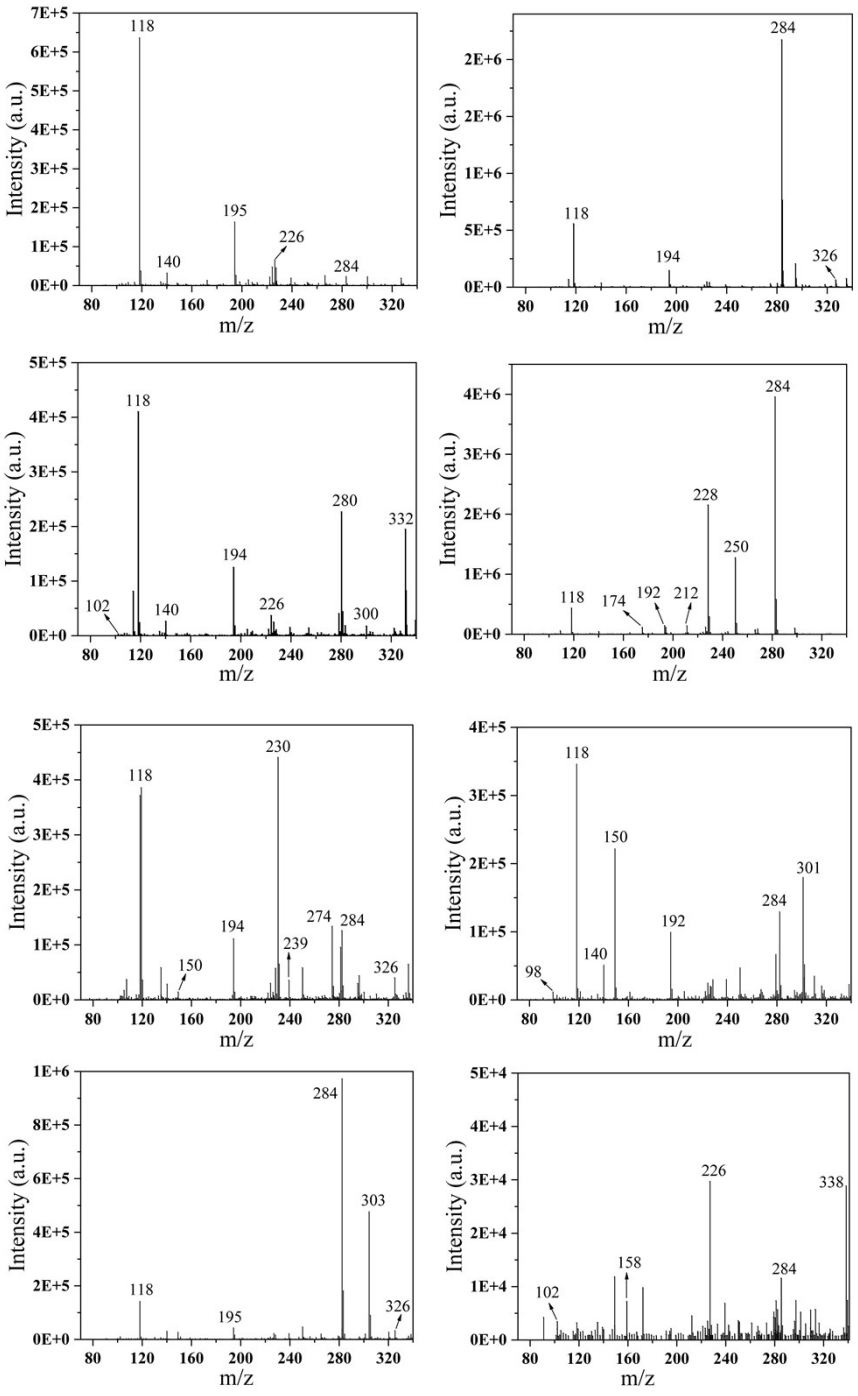

Fig. S6 LC-MS chromatograms for degradation intermediates of MB in the CuO@LDH-5 with H_2O_2 system.

References

[1] G.T. M. Frisch, H. Schlegel, G. Scuseria, M. Robb, J. Cheeseman, G. Scalmani, V. Barone, B. Mennucci, G. Petersson, Gaussian Inc., Wallingford, CT, USA, 2009.

[2] T. Lu, F.W. Chen, J. Comput. Chem., 2012, 33, 580–592.

[3] Z.Q. Cai, X.D. Hao, X.B. Sun, P.H. Du, W. Liu, J. Fu, Water Res., 2019, 162, 369–382.

[4] T.B. Nguyen, C.D. Dong, C.P. Huang, C.W. Chen, S.L. Hsieh, S. Hsieh, J. Environ. Chem. Eng., 2020, 8, 104139.

[5] L. Wolski, A. Walkowiak, M. Ziolek, Catal. Today, 2019, 333, 54–62.

[6] X. Kong, A.T. Chen, L. Chen, L. Feng, W.W. Wang, J. Li, Q.Y. Du, W.Z. Sun, J.T. Zhang, Sep. Purif. Technol., 2021, 272, 118850.

[7] H.A. Bicalho, J.L. Lopez, I. Binatti, P.F.R. Batista, J.D. Ardisson, R.R. Resende, E. Lorençon, Mol. Catal., 2017, 435, 156–165.

[8] H.L. Lu, L.L. Zhang, B.B. Wang, Y.D. Long, M. Zhang, J.X. Ma, A. Khan, S.P. Chowdhury, X.F. Zhou, Y.H. Ni, Cellulose, 2019, 26, 4909–4920.

[9] L. Wolski, M. Ziolek, Appl. Catal. B Environ., 2018, 224, 634–647.

[10] K.Y. Li, Y.Q. Zhao, C.S. Song, X.W. Guo, Appl. Surf. Sci., 2017, 425, 526–534.

[11] W.H. Li, X.F. Wu, S.D. Li, W.X. Tang, Y.F. Chen, Appl. Surf. Sci., 2018, 436, 252–262.

[12] R.X. Yang, Q.H. Peng, B. Yu, Y.Q. Shen, H.L. Cong, Sep. Purif. Technol., 2021, 267, 118620.

[13] C.Q. Wang, R. Huang, R.R. Sun, J. Mol. Liq., 2020, 320, 114421.

[14] R.G.L. Gonçalves, H.M. Mendes, S.L. Bastos, L.C. D'Agostino, J. Tronto, S.H. Pulcinelli, C.V. Santilli, J.L. Neto, Appl. Clay Sci., 2020, 187, 105477.

[15] X.Y. Liu, C. Sun, L.Y. Chen, H. Yang, Z. Ming, Y.T. Bai, S.C. Feng, S.T. Yang, Mater. Chem. Phys., 2018, 213, 231–238.

[16] X.F. Zhang, H.X. Wu, Z.Y. Ke, J.F. Yang, H.Z. Chen, F. Xue, E.Y. Ding, Water Sci. Technol., 2021, 83, 1834–1846.